Structural and paleomagnetic evidence for non-rotational kinematics of the South Pyrenean Frontal Thrust at the western termination of the External Sierras (southwestern central Pyrenees)

B. OLIVA-URCIA [1] **A.M. CASAS** [1] **E.L. PUEYO** [2] **A. POCOVI-JUAN** [1]

[1] **Departamento de Ciencias de la Tierra. Universidad de Zaragoza**
Pedro Cerbuna 12, 50009-Zaragoza, Spain. Fax: 976761106. Oliva-Urcia E-mail: boliva@unizar.es

[2] **Departamento de Geología y Geofísica del subsuelo. Oficina de Proyectos de Zaragoza IGME**
50006-Zaragoza, Spain

┤ **A B S T R A C T** ├

The definition of the structure and kinematics of the South-Pyrenean Frontal thrust, to the west of its westernmost outcrop in the External Sierras is the goal of this work. The methodology used is based on the construction and restoration of three balanced cross-sections. In addition to that, paleomagnetic analyses are applied to unravel possible vertical axis rotations linked to thrust kinematics. Stepwise thermal demagnetizations of 22 new sites together with previously published data from 25 sites (sampled in Bartonian-Priabonian sediments) define reliable primary directions in the region allowing for potential vertical axis rotations estimation. The comparison between the deformed and the pre-deformational states in the cross-sections agrees with the paleomagnetic data in that neither gradient of shortening, nor significant vertical axis rotations can be invoked to explain the along-strike changes of the main structures (folds and thrusts) linked to the South-Pyrenean Frontal thrust, west of the western termination of the External Sierras. Therefore, these changes are here interpreted as the result of a wedge thrust in the Paleozoic basement, the displacements of which are transferred to the Mesozoic-Tertiary cover through the Upper Triassic detachment level. This non-rotational kinematics of deformation implies a change of deformational style with respect to the External Sierras, where clockwise vertical axis rotations and gradient of shortening linked to rotational kinematics are found to be controlled by the Upper Triassic detachment level.

KEYWORDS │ Non-rotational. South-Pyrenean Frontal thrust. Vertical Axis Rotations. Gradient of shortening. Balanced and restored cross-section. Paleomagnetism.

INTRODUCTION

The External Sierras represent the frontal part of the Pyrenean fold and thrust belt, west of the South-Pyrenean Central Unit (see *e.g.* Capote *et al*., 2002). The subsurface structure of the South-Pyrenean Frontal thrust to the west of the western termination of the External Sierras (Santo Domingo anticline) has been interpreted in different ways (Fig. 1), partly because of the lack
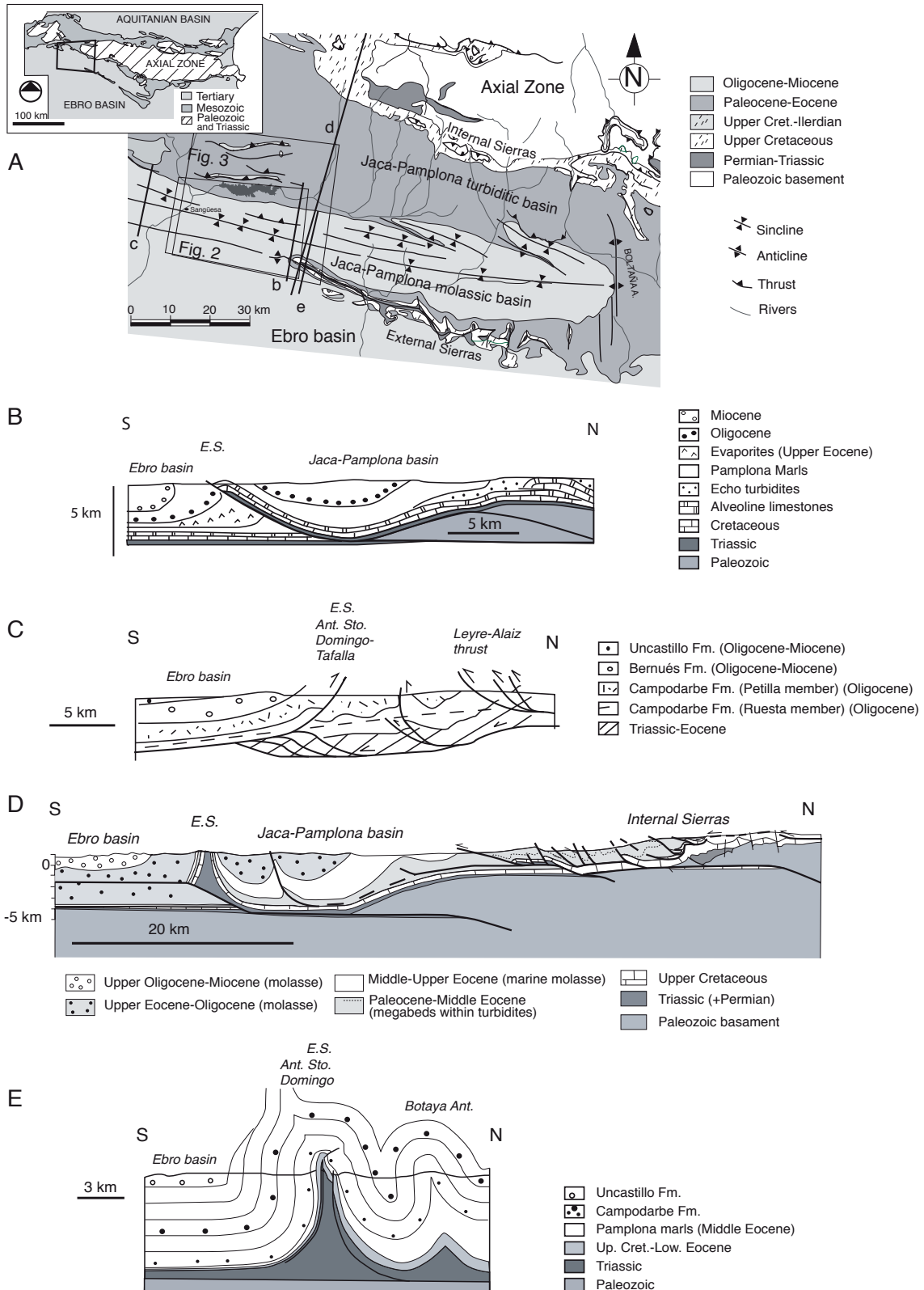
FIGURE 1 | A) Geological map of the Jaca-Pamplona basin (modified from Puigdefàbregas, 1975 and Millán, 1996). The lines are the cross-sections shown below, with the different structural interpretations for the External Sierras: B) Cámara and Klimowitz (1985). Cross-section 10km east of the Isuerre-Burgui cross-section. C) Turner and Hancock (1990) cross-section, 15km to the west of the Sangüesa-Epároz cross-section. D) Teixell and García Sansegundo (1995) cross-section, 10km east of the Isuerre-Burgui cross-section. E) Millán *et al.* (1995a) cross-section, 10km east of the Isuerre-Burgui cross-section.

of reliable subsurface data (seismic reflection profiles). Early interpretations (Cámara and Klimowitz, 1985) oversimplify the structure of the mountain chain, suggesting that the main structure is a basement frontal thrust (Guarga thrust) that crops out at the core of the External Sierras, superimposing Mesozoic-Tertiary cover materials over the Ebro foreland basin sediments. Nichols (1987) and Turner and Hancock (1990) proposed a backthrust incorporated into a triangle zone at the frontal area to explain some of the complexities appearing at surface. More recent interpretations (Teixell and García-Sansegundo, 1995; Teixell, 1996) propose a detachment of the Mesozoic-Tertiary sedimentary cover by an underlying thrust ramp. This ramp does not emerge to the surface, and may continue as a horizontal, buried detachment within the Tertiary sequence. However, there is not additional evidence for this buried detachment except for gentle folds involving the Uncastillo Formation (Fm.) South of the External Sierras (Teixell, 1996). Finally, Pocoví *et al.* (1990), Millán *et al.* (1992, 1995a) and Millán *et al.* (2000) proposed that the Santo Domingo anticline is a large WNW-ESE trending detachment fold, which deforms the Mesozoic-Tertiary cover. The core of this tight (almost isoclinal) anticline hosts a thrust she*et al*ong the hinge with a hanging wall movement to the south. The Middle-Upper Triassic (Keuper Germanic facies) is the main detachment level, with more than 500 m in thickness. In its westernmost sector, the axis of the Santo Domingo anticline plunges 60º westwards (San Marzal pericline).

In relation to rotational kinematics, early palinspastic reconstructions based on the distribution of paleocurrent orientations in the Jaca molasse basin (Puigdefàbregas, 1975) near its contact with the External Sierras, proposed a clockwise rotational emplacement for the South-Pyrenean Frontal thrust in the western sector of the External Sierras. Cross section balancing and restoration and derived shortening estimates (Cámara and Klimowitz, 1985; Nichols, 1987; McElroy, 1990; Millán, 1996; Millán *et al.*, 1992, 2000) in different transects in the External Sierras and the Jaca-Pamplona basin, also support rotational kinematics for the South-Pyrenean Frontal thrust. Magnetostratigraphic (Burbank *et al.*, 1992; Hogan and Burbank, 1996) and paleomagnetic (Pueyo *et al.*, 1999, 2002, 2003a, b, 2004) studies have addressed this problem during the last two decades and have contributed to accurately determine the amount, age and kinematics of the above-mentioned clockwise rotation. The southward displacement of the South-Pyrenean Frontal thrust shows maximum values ranging between 33-44km in the east, and progressively diminishes westwards to 10-14km (Millán, 1996). The Santo Domingo anticline has been proposed as a pinning point for the displacement of the Mesozoic-Tertiary sedimentary cover (Millán *et al.*, 1992) and seems to be related to the westwards thinning of the Upper Triassic detachment level. To the west of the studied area, approaching the Basque-Cantabrian basin, constant

shortening estimates of about 15km and the absence of vertical-axis rotations characterize the Pyrenean front at both walls of the NNE-SSW, nearly vertical Pamplona fault (Larrasoaña *et al.*, 2003a, b).

The goal of this paper is to determine the structural and kinematic evolution of the area located to the west of the western termination of the External Sierras. The structural and paleomagnetic analysis of this sector and adjacent areas is key to understand the pattern of the lateral propagation of the South-Pyrenean Frontal thrust. Three balanced and restored cross-sections were built allowing for shortening to be estimated. The methodology used includes geological mapping and interpretation of previous maps (Puigdefàbregas, 1975; Faci *et al.*, 1997), aerial photographs and paleomagnetic analysis. Subsurface data come from the Sangüesa and Roncal boreholes (Lanaja, 1987). Unfortunately, the scarce seismic data from this area are not available or have poor quality and therefore are not useful to constrain the presented cross-sections.

GEOLOGICAL SETTING

The studied area covers a part of the Jaca-Pamplona basin (Fig. 1). This WNW-ESE elongated basin is limited to the north by the Internal Sierras and the Axial Zone, to the south by the External Sierras and the Ebro basin, to the east by the Boltaña anticline, and it reaches the Basque-Cantabrian basin in its westernmost side. The outcropping sediments mostly correspond to the molasse sequence (mainly of fluvial origin, Campodarbe and Bernués formations) in the southern part of the basin (Guarga synclinorium, Almela and Ríos, 1951) and the turbiditic deposits (Hecho Group, Mutti, 1984) in its northern part (Puigdefàbregas, 1975). The turbidites, deposited during Ypresian-Lutetian times, represent the oldest and deepest part of the foreland basin (Mutti, 1984). The accommodation space for the Hecho Group to be deposited was created by the subsidence of the marine platform due to the tectonic load related to the emplacement of the thin-skin and basement thrust sheets to the north of the trough (Larra thrust system and Lakora thrust, respectively, Teixell, 1992). The subsidence of the foreland northern margin allowed the onlapping turbiditic wedge to be deposited over the Paleocene carbonate platform (Labaume *et al.*, 1985; Teixell, 1992; Barnolas and Teixell, 1994; Millán *et al.*, 1995b).

The shortening of the basement to the south of the Axial Zone is about 26-88km (Teixell, 1996; Martínez-Peña and Casas-Sainz, 2003). Pyrenean compression resulted in the formation of the south Pyrenean Frontal thrust in the External Sierras and the piggyback final evolution of the Jaca-Pamplona basin. Deformation in the External Sierras began during the Early Lutetian in the eastern sector

and in Aquitanian times to the west (Millán *et al.*, 2000; Arenas *et al.*, 2001). Therefore, the Jaca-Pamplona basin was a thin-skin piggyback basin (Séguret, 1972; Cámara and Klimowitz, 1985; Ori and Friend, 1984) linked to the movement of a non-outcropping basement structure, the Guarga thrust sheet (Teixell, 1992). Sedimentation in the basin during the Eocene was progressively shallower, changing from turbiditic to marsh and deltaic environments and finally to fluvial and lacustrine systems at the beginning of the Oligocene. Final deformation events (Chattian-Aquitanian) turn to be younger towards the east of the External Sierras (Millán *et al.*, 2000).

Stratigraphy

The sediments cropping out in the External Sierras range from Triassic to Miocene. The oldest sediments in the area crop out at the core of the Santo Domingo anticline (Upper Triassic Keuper facies). Because of its role as the main detachment level (Almela and Ríos, 1951; Séguret, 1972) the thickness of this unit is difficult to determine, and it is considered to be about 500m (Millán, 1996). To the west, at the Sangüesa borehole the Lower Triassic sandstones (Buntsandstein facies) are 300m thick and directly overlain by Upper Cretaceous rocks (Lanaja, 1987). Consequently, this implies a westward thinning and pinchout of the Keuper facies. This pinchout may be constrained to a narrow zone since farther North (Roncal borehole, Lanaja, 1987) and West (Pamplona fault transect, Larrasoaña *et al.*, 2003a) the Upper Triassic evaporites are present.

The Upper Cretaceous limestones overlying the Triassic are 100m thick and represent a widespread marine platform (Santonian-Maastrichtian; Mey *et al.*, 1968). These marine limestones are overlain by Garumnian continental facies (Tremp Group, Cuevas *et al.*, 1989), Late Cretaceous-Ilerdian in age, 60-100m thick in the External Sierras outcrops. Their equivalent to the Northeast are marine facies (Ager Fm., Luterbacher, 1969). The Guara Fm., deposited on top of the Garumn facies represents the foreland basin marine platform of Middle Eocene age (Puigdefàbregas, 1975). The top of the Guara formation is the Lutetian-Bartonian boundary (Canudo *et al.*, 1988). Its thickness diminishes from east (1000m) to west, with only 60m in its westernmost outcrop (Millán, 1996). To the north, the Guara Fm. limestones gradually pass to slope marls (Arro Fm.) and to the turbidites of the Hecho Group. Overlying the Guara Fm., external platform and prodelta deposits define the Arguis-Pamplona Fm., Bartonian in age. Younger deltaic and marsh sediments are represented by three units (Belsué Atarés, Yeste-Arrés and Guendulain Fms.) of Late Eocene age 2,600m in thickness (Teixell, 1996).

The youngest sediments (Oligo-Miocene) are of continental origin (detrital filling of the Jaca-Pamplona and Ebro basins) and cover most of the studied area (Campodarbe, Bernués and Uncastillo Fms., Soler and Puigdefàbregas, 1970; Puigdefàbregas, 1975; Montes, 1992). The lower fluvial and lacustrine sediments of these units (Campodarbe Fm.) show an E-SE provenance, later on changing to northern provenance (Bernués Fm., Puigdefàbregas, 1975). The Campodarbe Fm. increases its thickness westwards in the studied area (from 3,500m to ca. 7,000m; Puigdefàbregas, 1975). Several magnetostratigraphic profiles in the Campodarbe Fm. bracket its age between 29.0Ma (Rupelian) and 36.6Ma (Priabonian) and the Arguis–Guara Fms. boundary can be established at 41.52Ma (Hogan, 1993; Hogan and Burbank, 1996; Pueyo *et al.*, 2002).

CROSS-SECTIONS WEST OF THE EXTERNAL SIERRAS

The general structure of the studied area comprises three main structural domains: i) to the South, the westwards continuation of the South-Pyrenean Frontal thrust, resulting in several tight folds complicated by large-scale hinge collapses and intra-formational detachments; ii) a complex monocline that connects the southerly dipping marine deposits of the Jaca- Pamplona turbiditic basin to the continental deposits of the Jaca-Pamplona molasse basin and the Ebro basin, also with dominant southwards dips; iii) a structural high with outcrops of Upper Cretaceous involved in the thin-skin Leyre-Illón thrust system. The first zone, where much of the deformation is concentrated, can be divided into four parts (Fig. 2): 1) broad synclines in the northern border of the area (Rocaforte syncline in the west and Bailo syncline in the east), 2) tight anticlines in its central part (Botaya and Sangüesa anticlines), 3) minor folds to the south of zone 2, and 4) the anticline separating the Jaca-Pamplona basin from the Ebro basin, west of the westernmost outcrop of the South-Pyrenean Frontal thrust: the Santo Domingo-Tafalla anticline (Tafalla anticline in Puigdefàbregas, 1975) that can be followed more than 45km along trend. Immediately to the south of this fold there is a south-verging asymmetric syncline linking this area to the horizontal beds of the Ebro basin. The contact between the two basins is considered to be at places the stratigraphic contact between the Campodarbe Fm. (Jaca-Pamplona basin) and the Uncastillo Fm. (Ebro basin) (Puigdefàbregas, 1975, Arenas, 1993). The two structures that can be followed along strike throughout the studied area are only the Santo Domingo-Tafalla anticline in the south and the southward-verging Leyre-Illón imbricated thrust system to the north (Fig. 3). Geological maps and cross-sections focused on the structure of the Campodarbe Fm. (Fig. 2) indicate relay of fold axes along trend, with an increase in the number of folds toward the west along with the increase in thickness

FIGURE 2 | Geological map and photogeological interpretation of bed contours in the central part of the Jaca-Pamplona basin.

of the unit (Oliva *et al*., 1996, 2000). This is consistent with the behavior of multilayer folding, which depends, among other parameters, on the number and thickness of the layers and their mechanical strength (Ramberg, 1963; Frehner *et al*., 2006).

The three cross-sections presented in this work have a SSW-NNE direction, perpendicular to the dominant structural trend (Fig. 3). The horizontal base level for cross-section balancing is the top of the Campodarbe Fm. (Upper Eocene-Lower Oligocene). Both the thickness and length of the layers are maintained in the balanced and restored cross-sections, since no cleavage or continuous deformation is found in this area. Footwall ramp angles in the basement at the thrust fronts have been calculated considering the fault-bend geometrical model (Suppe, 1983), although there are not reliable data about the deformation style at depth.

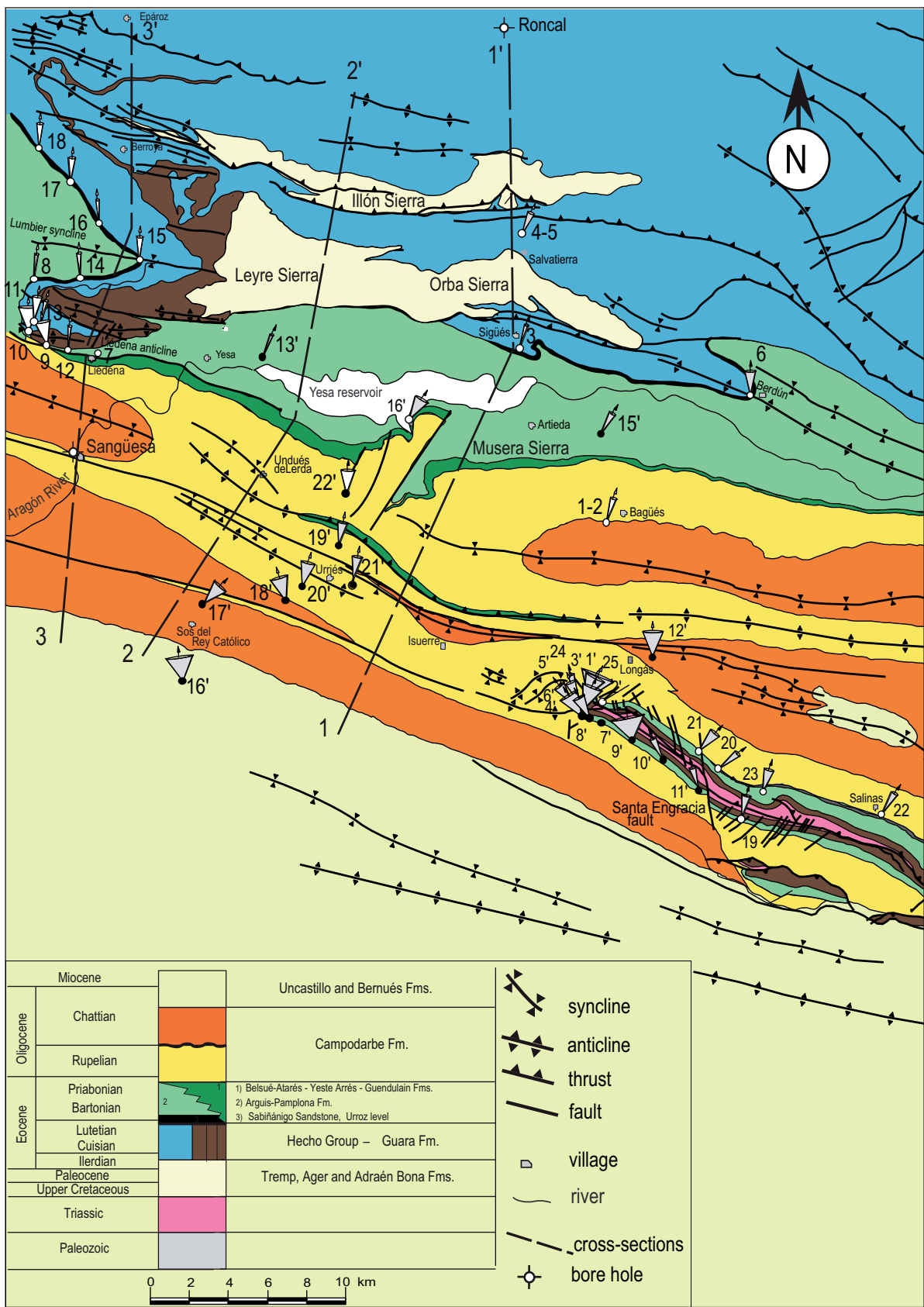## Isuerre-Burgui cross-section (1-1')

The southern part of this cross-section (Fig. 4) shows the continuity of the Santo Domingo-Tafalla anticline to the west of the External Sierras. We interpret that the anticline is linked at depth to a north verging blind thrust rooted in the Upper Triassic evaporites. The thrust cuts across the anticline hinge affecting from Triassic rocks to the lower part of the Campodarbe Fm. The amplitude of the Santo Domingo-Tafalla anticline decreases from E to W, in the same direction of the plunge of the fold axis. The anticline has a westerly plunge of 60° and its amplitude is around 4km in San Marzal (western termination of External Sierras, Pueyo *et al*., 1994), whereas in this section its amplitude is 2km. At the surface, it appears as a tight fold involving the Campodarbe Fm., with layer-parallel slip. As a result, hinge collapse occurs (saddle reef structures, Ramsay, 1974). Hinge collapses are typical in multilayer systems when kink-type folds occur (Ramsay, 1974). To the north, the asymmetric Longás syncline shows a southward vergence. The South-verging Botaya thrust, which has an anticline in its hangingwall, cuts the northern limb of this syncline. The northern limb of the Botaya anticline is the southern limb of a broad syncline (Bailo syncline), slightly verging to the South. The sedimentary wedge composed mainly by the Hecho Group and the Arguis-Pamplona Fm. thickens from the Bailo syncline towards the north. In the northern limb of the Bailo syncline, marine platform Mesozoic-Tertiary materials crop out, defining an imbricated thrust system (Lere-Illón) rooted in the Upper Triassic detachment level. These thrust sheets have individual displacements up to 2km approximately, and a general southward vergence, although bi-vergent anticlines can be found at surface, forming pop-up structures in the hangingwalls of thrusts.

Sos del Rey Católico-Undués de Lerda cross-section (2-2')

In this cross-section (Fig. 5) the Santo Domingo-Tafalla anticline shows a similar geometry to the previous cross-section, with a well-developed triangle zone below the Longás syncline: the Botaya thrust, with southward vergence, is interpreted to cut the blind back-thrust. At surface, the continuation of the Santo Domingo-Tafalla anticline shows similar amplitude as in the previous section, although the throw of the thrust with northward vergence is higher in this section. To the north, the structure continues in the Urriés anticline, with short continuity along trend (Fig. 2). A hinge collapse can be inferred from photogeological analysis in the eastern termination of this anticline, as a consequence of layer-parallel slip. The Longás syncline connects with the Urriés anticline to the south and the Botaya anticline to the north. The Botaya anticline has lower amplitude (from around 3km in section 1-1' to 1km in this one). The thrust associated with the Botaya anticline shows lower displacement in this central section (few hundreds of meters). The continuation of the cross-section to the North is very similar to cross-section 1-1', except for the larger displacement of thrusts (up to 7km) in the Leyre-Illón thin-skin thrust system. The sedimentary wedge of the Hecho group and Arguis-Pamplona Fm. is interpreted to thicken to the north of the Botaya anticline, as in section 1-1'.

Sangüesa-Epároz cross-section (3-3')

This cross-section cuts across the Sangüesa borehole (Lanaja, 1987) which exposes the real thickness of the formations and confirms the pinchout of the Upper Triassic (Fig. 6). The accommodation of the shortening involves a north-verging intra-formational detachment in the Campodarbe Fm. that continues into the Ebro basin as a minor buried detachment. At surface, the Santo Domingo-Tafalla anticline is still observed and shows a northerly vergence, although both its amplitude and wavelength are smaller than in the central cross-section. The detachment developed at its hinge due to layer parallel slip is slightly smaller than in section 2-2'. The core of the anticline is interpreted in this section to be detached within the marls and anhydrite levels located within the Eocene sequence found in the Sangüesa borehole. To the north, the tight Sangüesa anticline has a southerly vergence and layer-parallel slip also occurs. Further north, the Rocaforte syncline shows an unconformity in the Campodarbe Fm. (León, 1985), indicating its Eocene-Oligocene age. This gentle fold with southern vergence is bounded by the Loiti fault on its northern limb, wich we interpret as a folded reverse fault with northern vergence that represents the boundary between the molasse and the turbiditic sequences of the Jaca-Pamplona basin. It is cut by the south-verging

FIGURE 3 | Geological map with the location of the cross-sections shown in Figures 6, 7 and 8. Stratigraphic column (modified from Puigdefàbregas, 1975; Millán, 1996). Location of the studied and previous paleomagnetic sites.
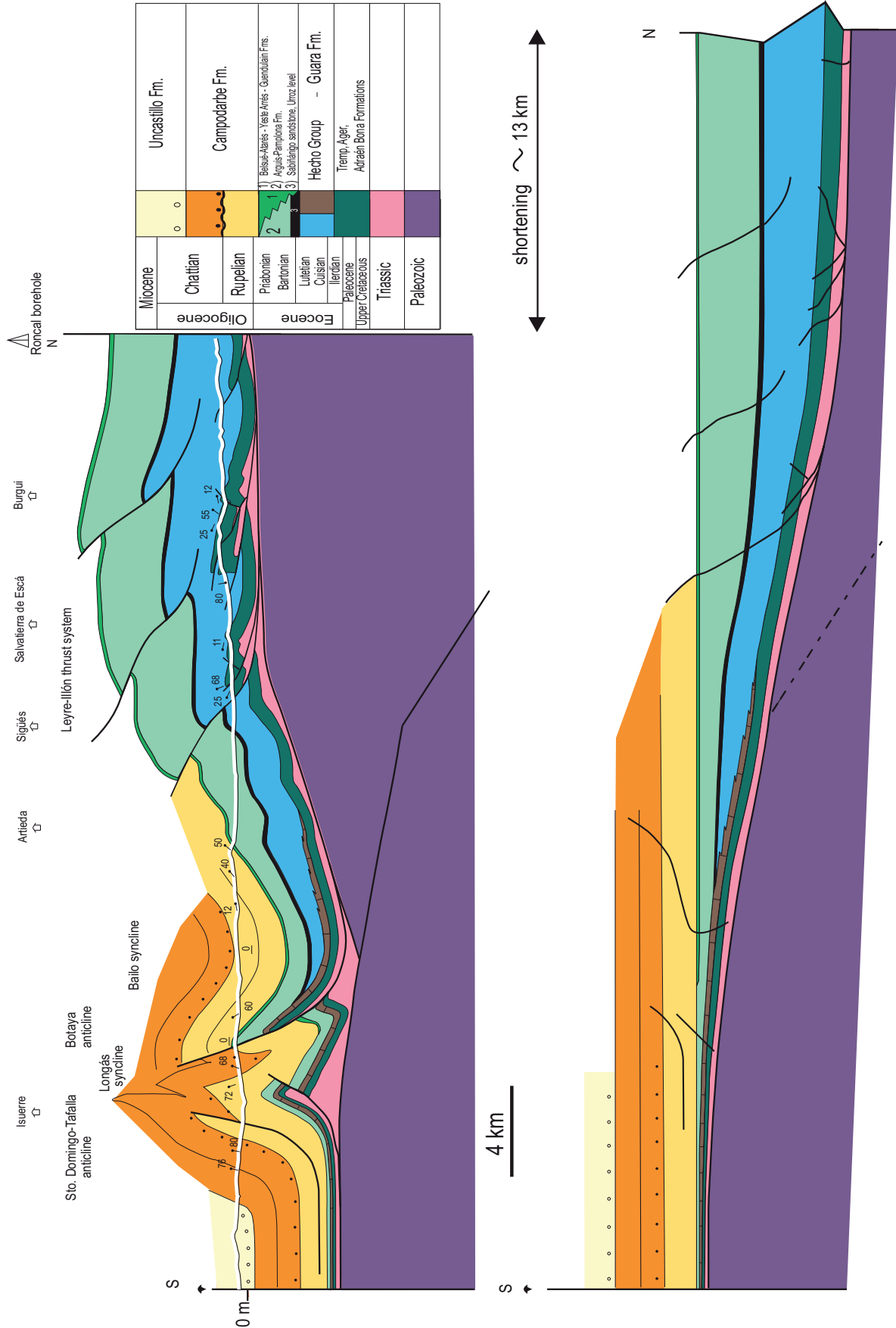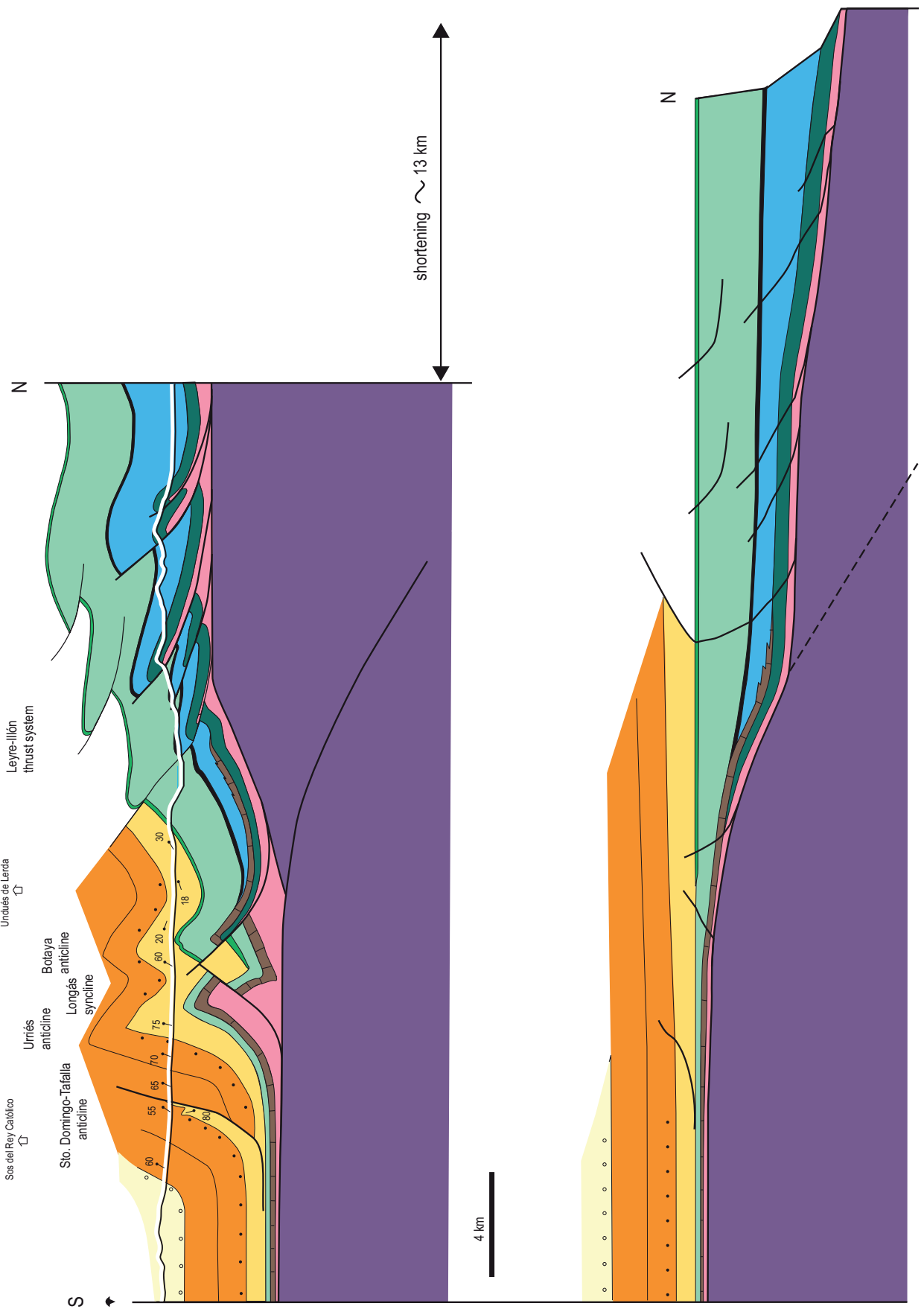
FIGURE 4 | Isuerre-Burgui geological cross-section and the corresponding restored section (1-1').

FIGURE 5 | Sos del Rey Católico-Undués de Lerda geological cross-section and the corresponding restored section (2-2').

sole thrust associated with the Leyre-Illón imbricated thrust system. According to this interpretation, the Loiti fault and the southernmost imbricated thrust sheet define a narrow triangular zone.

Compressional structure of the Paleozoic basement

Several constraints must be taken into account when interpreting the structure of the Paleozoic basement below the structures described in the three cross-sections:

1) The gradual descent of the base of the Mesozoic sequence from North to South, with an average dip of 10-15º, and the different elevation (about 2000m) of the reference levels (Upper Cretaceous) between these two areas.

2) The practical absence of cleavage or ductile deformation at surface in the area represented in Fig. 2.

3) The existence of a widespread detachment level (except for the southern part of section 3-3') that allows for shortening and deformation at the basement and cover levels to be distributed in different structures.

According to these constraints, the structure of the Paleozoic can be interpreted as a south-verging wedge thrust including a ramp-flat transition in its footwall and a hangingwall anticline. The weak southward dip of the front limb of the hanging wall anticline can be explained as a result of the northward-opening wedge in the Tertiary sequence, driven by foreland basin evolution and crustal flexure towards the North. Assuming a maximum dip for thrust surfaces of 30-35º, the wedge angle of the hangingwall in its leading edge should initially be 20-25º. This gives a footwall ramp angle of 25-30º for an interlimb angle between 155-160º (see Suppe, 1983). However, the depicted geometry differs from the flat-ramp-flat model in the footwall flat lacking in the hinterland, thus precluding the formation of a hangingwall syncline at the backlimb.

The thrust displacement necessary to account for the ramp-flat transition and hangingwall fault-bend folding in the Paleozoic is between 11 and 13km in the three sections. This amount of shortening in the Paleozoic is accommodated in the Mesozoic-Tertiary cover by means of folds, back-thrusts and thin-skin thrust sequences, favored by the Upper Triassic detachment level. In cross-section 3-3 the Upper Triassic disappears towards the South (Sangüesa borehole), but a level of breccia between the Tertiary marine limestones and the Triassic red beds can indicate the presence of a detachment between the Paleozoic and the Tertiary cover. An alternative interpretation could favor the décollement between the basement and the cover within the Eocene evaporates found below the continental Tertiary deposits in the Sangüesa borehole.

The critical issue is that, in spite of the lateral variations in the structure of the basement, shortening is similar in the three sections. This indicates that no significant vertical axis rotation can be predicted in the area during the Pyrenean compression. The new and previously published paleomagnetic data discussed in the next section can be used to evaluate this prediction.

Paleomagnetic sampling and procedures

Twenty-two new paleomagnetic sites are presented in this work (Table I). They are interpreted together with previously published data from 25 additional sites (Hogan and Burbank, 1996; Larrasoaña *et al.*, 1996; Larrasoaña *et al.*, 2003a; Pueyo *et al.*, 2003a; Pueyo *et al.*, 2004) (Table I). Every new site consists of 7-10 standard cores spanning along 3-10meters of stratigraphic pile and sharing an equal bedding attitude. Cores were drilled with a portable water-refrigerated machine and directly oriented in the field with an inclinometer. Sampling was designed to obtain robust fold tests in structures at a regional scale. 14 sites of the new locations were drilled in the blue marine marls and transitional sandstones (Arguis-Pamplona Fm. and Liédena Fm.) Bartonian to Priabonian in age, the other 8 sites come from the Oligocene-Miocene Campodarbe and Bernués alluvial Fms. (reddish sandstones and shales). The study area was divided into three different domains to address the structural interpretation (see numbers in Table I): 1) The northwestern part of the Jaca-Pamplona basin includes the Atarés anticline (north of the Bailo syncline, in the turbiditic basin, Puigdefàbregas, 1975) and the Bailo syncline and was interpreted together with data from the eastern Eocene Pamplona Basin (Izaga syncline and Liédena anticline, Puigdefàbregas, 1975; Larrasoaña *et al.*, 2003a); this dataset was sampled in Bartonian marine and transitional sediments. 2) The Cinco Villas, SO-sites (10km east of the Sangüesa-Epároz section presented above, comprise data from the Tafalla, Botaya and Urriés anticlines all obtained in rocks of the Campodarbe Fm. (Jaca-Pamplona molasse basin). 3) Finally, the western termination of the External Sierras frontal thrust includes data from the southern flank of the Santo Domingo anticline (Santo Domingo-sites), the San Marzal pericline (San Marzal-sites) and previous paleomagnetic sites in the northern limb of the fold (Pueyo *et al.*, 2003a; b). In this last case, the entire data set was located at the Bartonian marls (Arguis Fm.).

Rock magnetic analyses were done to characterize the remanence carriers at the Institute for Rock Magnetism (University of Minneapolis). Hysteresis loops and thermal runs were done in the micro-vibrating sample magnetometer (Princeton), and low temperature essays
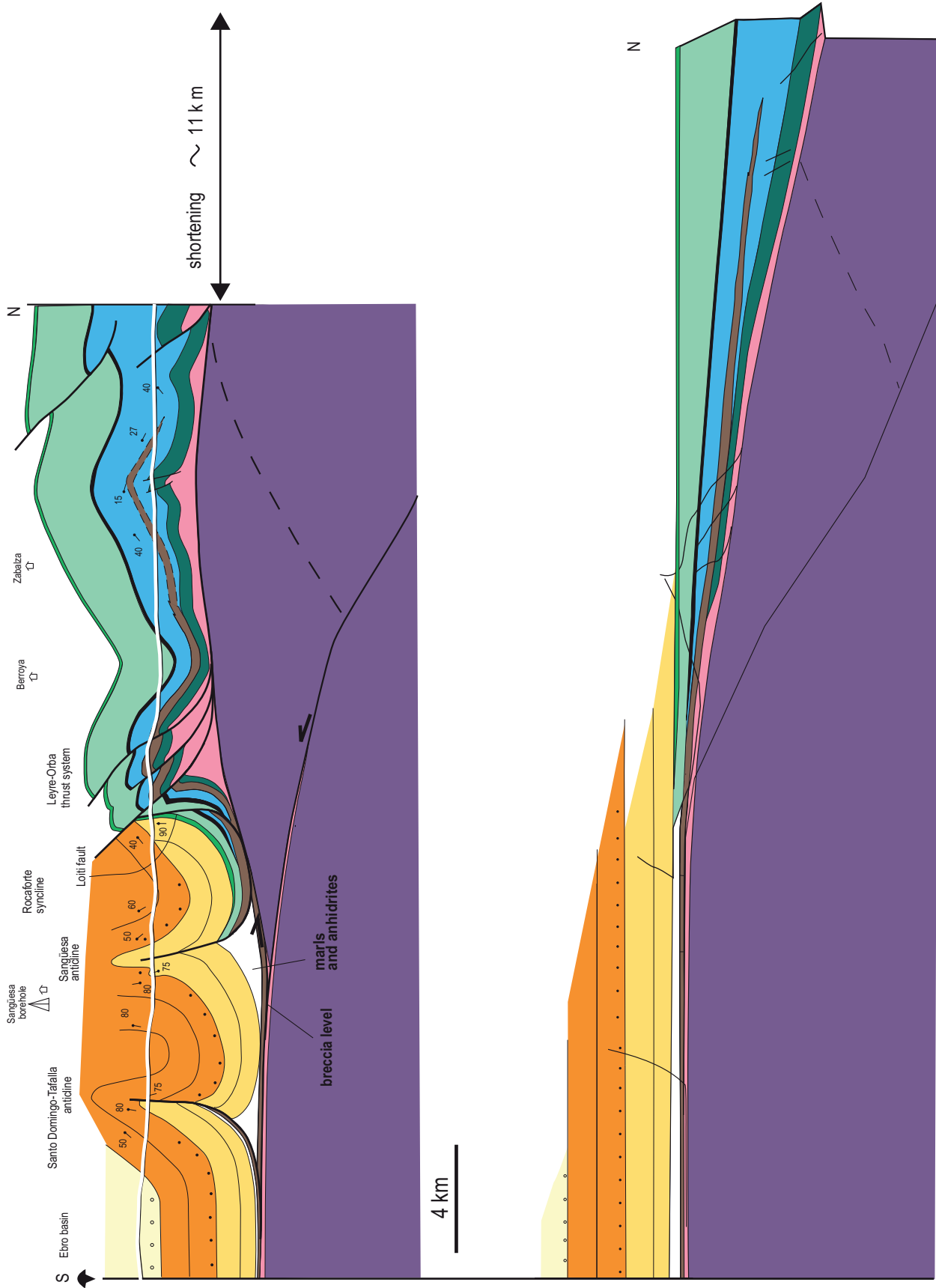
FIGURE 6 | Sangüesa-Epároz geological cross-section and the corresponding restored section (3-3').

(both magnetic remanence and induction) in the magnetic properties measurement system (Quantum Design). Stepwise thermal demagnetizations were successfully applied to separate magnetic components in most samples every 25°-50°C intervals. Measurements were performed in two laboratories with shielding room capabilities (Lodestar): the Albuquerque paleomagnetic laboratory (University of New Mexico) and at the Pastel group (University of Michigan at Ann Arbor). Magnetization measurements were taken by 2G 3-axes superconducting quantum interference device magnetometers, and thermal treatment was applied by means of TSD-1 oven (Schonsted) at Albuquerque and by a TD-48 furnace (ASC company) at Ann Arbor.

Data processing and reliability

Paleomagnetic characteristic remanent magnetizations were fitted with "Paldir" software (Utrecht paleomagnetic laboratory) with a manual selection of points and principal component analysis (Kirschvink, 1980). The demagnetization-circles method (Bailey and Halls, 1984) and the stacking routine (Scheepers and Zijderveld, 1992; Ramón and Pueyo, 2008) were also applied to support poorly characterized site means. Fisherian statistics (α_{95} and k; Fisher, 1953) was used at the site scale. Intra-site comparisons, including the fold test (Super IAPD software by Torsvik *et al.*, 1996), were also performed to constrain the age of the magnetic components. Sites were carefully evaluated following the reliability criteria of paleomagnetic data (Van der Voo, 1993) and the occurrence of potential structural errors (adequate restoration, possible component overlapping and internal deformation) were also considered.

PALEOMAGNETIC DATA

Most sites (64%) shown in this work are from the Arguis-Pamplona marls Fm. with natural remanent magnetization intensities spanning around 50×10^{-6}A/m to 250×10^{-6}A/m. Low field and room temperature susceptibility (KLY-2) ranges around 150×10^{-6}S.I. Regardless of the major contribution of paramagnetic susceptibility at room temperature in the marly sites (always larger than 90% at low fields), a weak but stable signal is carried by ferromagnetic minerals seen in the hysteresis loops (Fig. 7A), which are magnetite (as seen with the Verwey transition, Fig. 7B) and iron sulphides as previously shown in Larrasoaña *et al.* (2003c). The Campodarbe and Bernués rocks display ten times larger initial magnetizations and, together with evidences of oxidized magnetite in the susceptibility dependence temperature (Fig. 7D), they show clear evidences of hematite as described in abundant magnetostratigraphic studies of the Jaca molassic basin (Hogan, 1993).

In the Arguis-Pamplona formation the thermal demagnetization was successfully applied to untangle the different natural remanent magnetization components (see Fig. 8): A) An unstable and viscous direction (present geomagnetic field, drilling and storage overprints) unblocking sometimes up to 200°C. B) The characteristic direction, unblocking between 250° and 450°C (sometimes even at higher temperature). The increase of susceptibility around 300-350°C precludes, in some cases, complete magnetic cleaning; nevertheless, this problem does not hamper the fitting of a ChRM with two polarities in most cases. Hard components in the Campodarbe formation show a different behavior and, besides the viscous component (sometimes up to 400°C), the ChRM unblocks between 300-400°C and 650-680°C (Fig. 8). At the sample scale, maximum angular deviations (from PCA, Kirschvink, 1980) do not reach 15°. Most sites (70%) display reasonable confidence angles ($\alpha_{95} < 15°$) for the mean vector. The stacking routine and the demagnetization circles results support the fisherian means; σ angles (maximum angular deviation between different means) do not usually exceed 15°.

Paleomagnetic Stability and reliability of data

The ChRMs are systematically defined in constant temperature intervals. It is considered as a primary direction since: 1) the fold test (McElhinny, 1964) is positive (Fig. 9A) as in previous works of the External Sierras (Pueyo *et al.*, 2002, 2003a, 2004), and the Pamplona basin (Larrasoaña *et al.*, 2003c). 2) The 22 new sites show two polarities after tectonic correction and they are antiparallel: they share a common mean at 95% confidence in the reversal test of McFadden and Lowes (1981) and the reversal test of McFadden and McElhinny (1990) is positive. In addition, there are positive reversal tests in marls of the Pamplona basin (Larrasoaña *et al.*, 2003c) and in the Campodarbe Fm. (Hogan, 1993). 3) The magnetic inclinations after tectonic restoration of the studied sites (except for LN01) are similar to the inclination of the Eocene reference for Iberia (D&I:005, 52, α_{95}:5; k:546).

DISCUSSION

Shortening and kinematics

The balanced and restored cross-sections allow for the shortening along the Pyrenean trend in different transects of the External Sierras to be estimated. The amount of shortening, both in the Mesozoic-Tertiary cover and the Paleozoic, is similar in the three sections presented (between 11 and 13km). This implies that the differential shortening found in previous works along the entire External Sierras front (Nichols, 1987; McElroy, 1990; Millán, 1996) and

the subsequent vertical axis rotations (Pueyo, 2000; Soto *et al.*, 2006; Oliva-Urcia and Pueyo, 2007a, b) cannot be applied farther west of the San Marzal pericline, where 11-13km of shortening is estimated. The non-rotational kinematics of the southernmost Pyrenean structures has also been assessed westward, in the Pamplona Basin by paleomagnetic analysis and cross section balancing at both sides of the Pamplona fault (Larrasoaña *et al.*, 2003a) accounting for 15km of uniform shortening.

The style of shortening depends on the mechanical stratigraphy of the pre-deformational sequence. On one hand, the Mesozoic cover and the marine platform limestones of Paleocene-Lower Eocene age, less than 2km thick, are cut by thrust sheets with relatively low displacement and folded with low amplitude and wavelength. On the other hand, the Campodarbe Fm., a thick (4-7km) homogeneous sequence, shows WNW-ESE folds with intra-formational detachments and hinge collapses due to the layer parallel slip typical of buckling in multilayer systems. Buckling produces folded layers with different tilting angles in relation to the thickness of the layer (Ramsay, 1974; Ramsay and Huber, 1987). Therefore, the hinge of competent layers breaks and
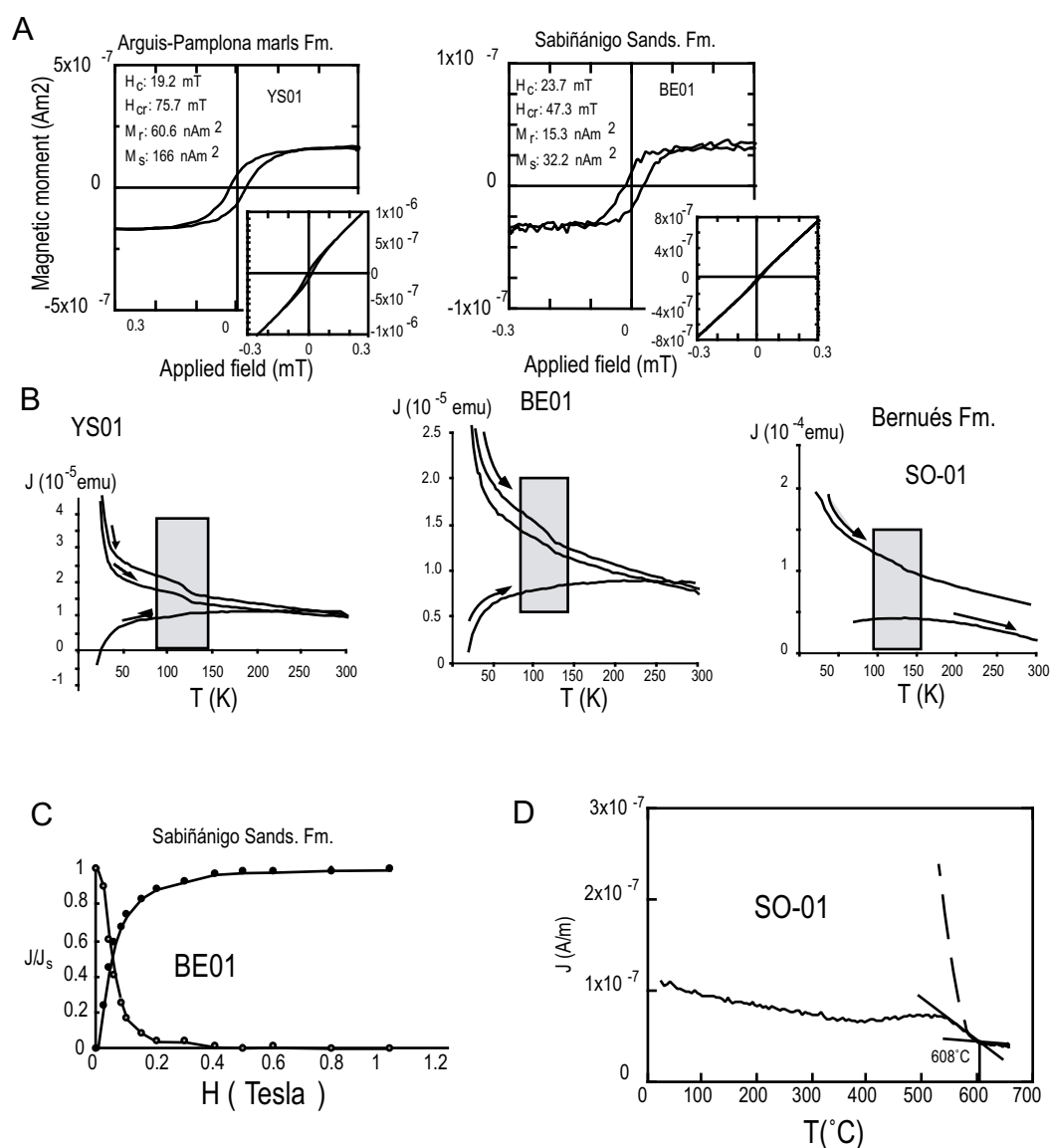
FIGURE 7 | Rock magnetism of selected samples of the southwestern Pyrenees. A) Hysteresis loops (before and after paramagnetic correction). B) Low temperature sweeping of remanent magnetization. C) Isothermal Remanent Magnetization. J/Js refers to normalized magnetization. D) Temperature dependent susceptibility (k-T curves) allow controlling the Curie temepratures (Tc) of ferromagnetic minerals, and hence to diagnose the ferromagnetic mineral present. In this case, the Tc is higher than 580ºC (the typical Tc for magnetite), indicating maghemite as the present mineral. Maghemite occurs probably by oxidation of magnetite.

collapses. This is observed at large scale in the anticlines involving the Campodarbe Fm.: Santo Domingo-Tafalla, Urriés, Botaya and Sangüesa. Nevertheless, according to the interpretation proposed in our cross-sections some of the folds in the Campodarbe Fm. involve the whole sedimentary

sequence located above the detachment level, although their geometry changes along the sedimentary pile.

The geometry represented in the cross-sections implies that the basement shortening is balanced with the shortening
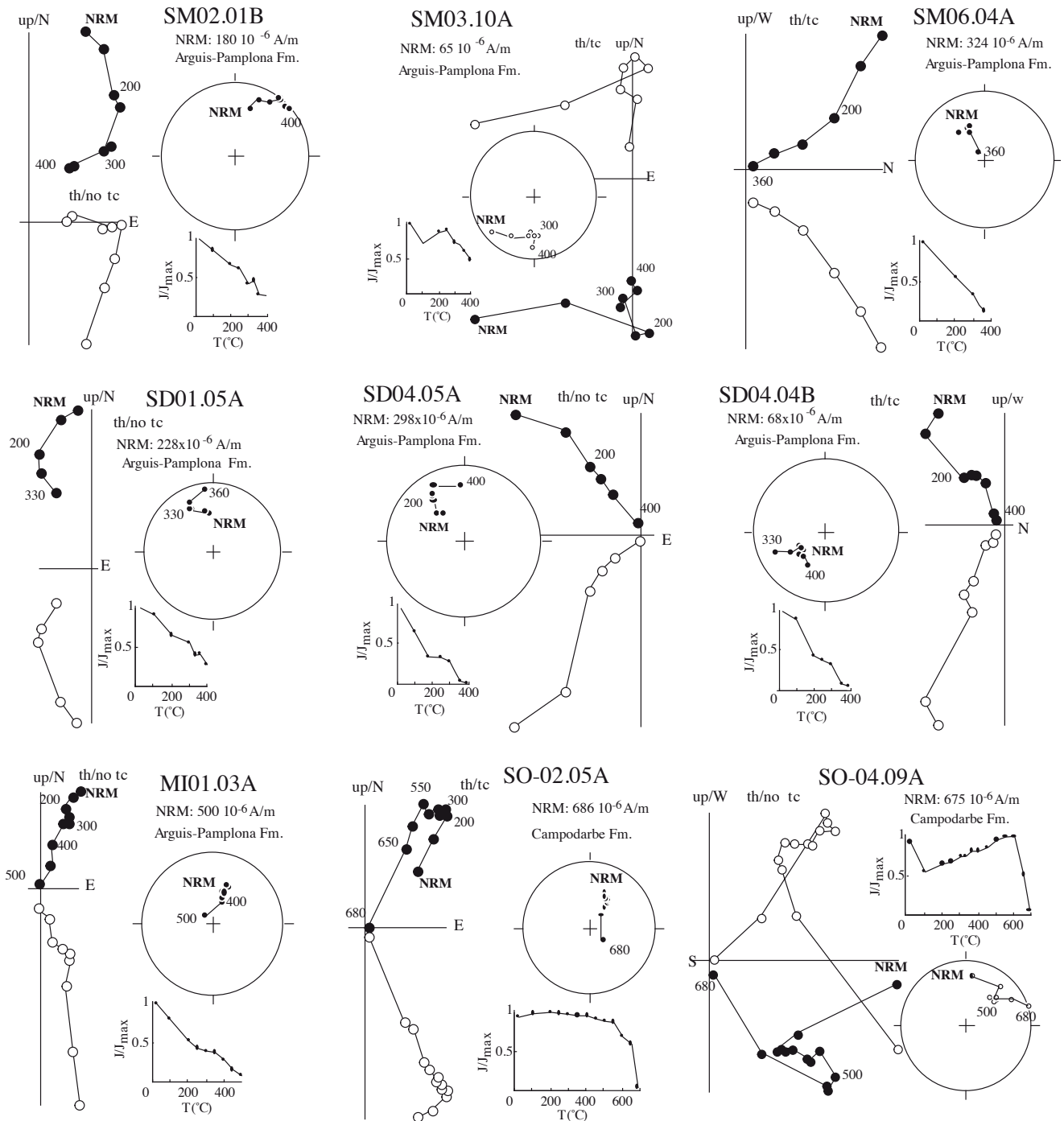
FIGURE 8 | Orthogonal diagrams, stereonet projections and decay of the remanence for stepwise thermal demagnetizations of selected samples in the western Sierras. White dots: upper hemisphere projection. Black dots: lower hemisphere projection. Orientation of orthogonal projection indicated by up/N and up/W. th: thermal demagnetization. tc: tectonic corrected. no tc: no tectonic corrected. J/jmax: normalized magnetization at every step. NRM: natural remanent magnetization.

of the Mesozoic-Tertiary cover, having both thrust systems connected through a wedge thrust. A consequence of this new structural interpretation is that the shortening related to the Gavarnie thrust is represented north of these cross-sections or can be considered to involve the sediments of the turbiditic basin without reaching the Upper Triassic in this area. However, it is important to remark that the thrusts of the Leyre-Illón system pass laterally in the eastern Jaca basin into folds that show evidence of Late Eocene-Early Oligocene activity (*e.g.* contemporary with the Gavarnie thrust, cf. Teixell, 1996). Therefore, this thrust system could be initiated before the extensive displacement of the basement thrust which, in our opinion, accounts for most of the fault slip in the post-Triassic sedimentary cover. Another consequence of our structural hypothesis is that it contradicts previous interpretations (Millán *et al.*, 2006) since the shortening related to the Guarga thrust sheet in the area we studied here is related to the slip along the thrust fault, whereas in the eastern sector of the External Sierras, shortening of the Guarga thrust sheet has been previously interpreted to be related to the internal deformation of the basement, with very little slip along the thrust fault (5km) and thickening of the basement rocks in the hangingwall due to flattening (8km) (Millán *et al.*, 2006). Due to the lack of evidences for internal deformation and flattening in the basement rocks we propose a new structural interpretation for the development of shortening in the western termination of the External Sierras. In addition, this new interpretation also disagrees with previous explanations related to the southern end of the Guarga thrust sheet (Teixell and García Sansegundo, 1995; Teixell, 1996, 1998). These authors interpret that the Guarga thrust sheet ends as a blind thrust in the Tertiary molasse after ramping up half of the Tertiary continental deposits of the Ebro basin. Again, our interpretation of the shortening accommodation differs, since we constrain the deformation to the studied area, where there is little deformation in the northern margin of the Ebro basin. In our interpretations we consider that i) the southward displacement of the basement thrust sheet cannot be consumed in structures located farther south (since in the transect presented no structures can be found in this sector of the Ebro Basin) and ii) layer parallel shortening within the Tertiary deposits cannot account for the fault slip determined by the movement of the thrust sheet within the Tertiary sequence at the front of the External Sierras (more than 15% of strain would be required on average in a sequence that is apparently not deformed). Therefore, a sharp change can be established between this area and areas located farther East and West (Fig. 10) where displacements can be transferred to the South by means of evaporite levels within the Tertiary sequence of the Ebro basin, or as a wholesale displacement of the Mesozoic-Tertiary cover favored by the Upper Triassic detachment level.

Rotation magnitudes

The paleomagnetic data is grouped in five regional sectors (Fig. 11) to discuss the vertical axis rotations since these rotations are very variable, ranging at site scale from +45º to -40º, Table I, Figures 3 and 11.

In the External Sierras we distinguish three sectors, the northern limb, the southern limb and the western termination of the External Sierras (San Marzal pericline). In the northwesternmost portion of the External Sierras there is a clockwise rotation higher than +40° (see Table I, Fig. 11), agreeing with the estimates given by simple geometrical models (Millán *et al.*, 1992). However, the southern limb of the Santo Domingo anticline displays an unexpected counterclockwise rotation value of about -17º. Therefore the western sector of the External Sierras are able to accommodate more than +60° of bulk rotation during their formation (larger than previously predicted). The counterclockwise rotation in its southern flank contrasts with the overall moderate clockwise rotation detected all along the 100km External Sierras front (25-30°). The counterclockwise rotation dies out to the south in the Agüero, San Felices and Ayerbe profiles (D&I:359, 37; (alpha 95) α_{95}:4.1°; K:5.3; n:271) of the Uncastillo Fm. (Hogan, 1993) and it also disappears along-strike of the Santo Domingo southern limb to the East (Santa Engracia fault, between sites 11' and 19 in Fig. 3), since
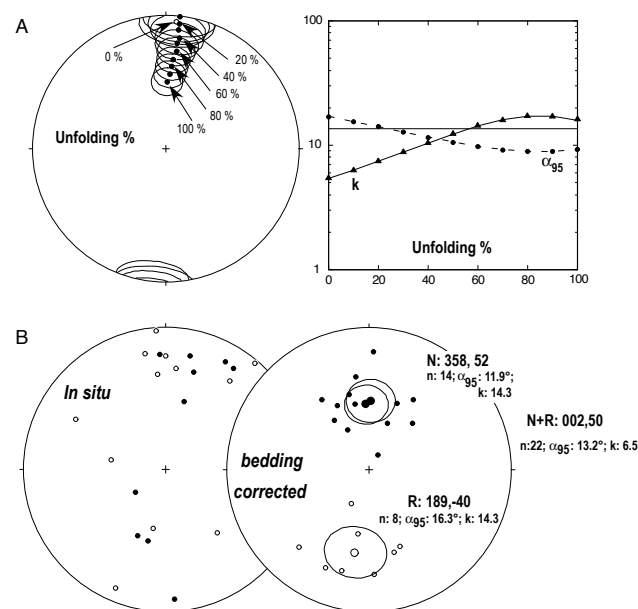

FIGURE 9 | Orthogonal diagrams, stereonet projections and decay of the remanence for stepwise thermal demagnetizations of selected samples in the western Sierras. White dots: upper hemisphere projection. Black dots: lower hemisphere projection. Orientation of orthogonal projection indicated by up/N and up/W. th: thermal demagnetization. tc: tectonic corrected. no tc: no tectonic corrected. J/jmax: normalized magnetization at every step. NRM: natural remanent magnetization.

significant rotations are not found in this sector within the Eocene marls (Pueyo *et al.*, 2003a, b). Consequently this Counter clockwise (CCW) rotation seems to be a local effect probably caused by the pinning of the fold and the impossibility for the northern limb to accommodate more rotation.

In the San Marzal pericline, there is no rotation, as seen in Fig. 11. This average involves sites with clockwise rotations (northern limb of the pericline) and counterclockwise rotations (southern limb Fig. 11).

The northwestern part of the Jaca-Pamplona basin is summarized in Fig. 11 as Leyre-Illón ranges. This sector displays moderate Clockwise rotations (~19°) similar to those obtained in the Internal Sierras (Oliva-Urcia and Pueyo, 2007a, b). However, these values differ both to the important clockwise (CW) rotation of the northern flank of the Santo Domingo anticline (≈ 40-45°) and to the undetectable rotation values found to the west of the Sierra de Leyre (Lumbier syncline and Liédena anticline, location in Fig. 3) and in the entire Pamplona basin (Larrasoaña *et al.*, 2003a, b).

Finally, the Cinco Villas section (SO sites) with lower quality of paleomagnetic results in the detrital Campodarbe Fm., shows a mean value without significant rotation (D&I:003,29; (alpha 95) α_{95}:15; k:20). These data are also in agreement with the absence of rotations in sites more to the west in the Pamplona basin (Larrasoaña *et al.*, 2003a).
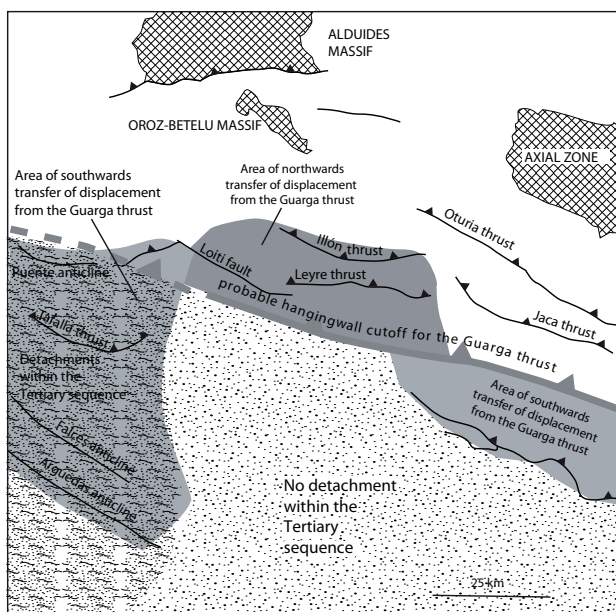
**FIGURE 10** | Conceptual model of displacement transfer for the studied area.

Chronology of rotation and deformation

The Santo Domingo anticline could be nucleated during Eocene-Oligocene times at the time of the formation of the External Sierras imbricated system. However, the present geometry of the structure was definitively formed during Miocene times, after the sedimentation of the Campodarbe and Bernués Fms. (Millán, 1996). During this time a large amount of rotation was accommodated in the External Sierras. Averaged out rotations are significant (≈30° CW) along the Salinas section during Oligocene time (Hogan and Burbank, 1996; Pueyo, 2000) and seem to be significant until Late Rupelian (Miocene) times (at least C10r) proving a coeval rotational and folding event.

Westward change of structural style in the External Sierras

The data presented in this work indicate that no important regional rotation occurs west of the western end of the External Sierras, in spite of seemingly rotational structures linked to conical, plunging folds and pinchout of the main detachment level. This apparent contradiction can be explained taking into account a wedge thrust geometry in the Paleozoic basement and transfer of displacement to the Mesozoic-Tertiary cover located in the hangingwall. East of the studied area, the southward displacement of the Guarga basement thrust is transferred to structures located farther South (between 5 and 25km, see cross-sections in Millán, 2006) in the Mesozoic-Tertiary cover (Fig. 10). West of the studied area the displacement of the Guarga thrust is probably consumed in structures décolled within the Eocene sequence (see *e.g.* Casas *et al.*, 1994; Faci *et al.*, 1997). In the studied area the displacement of the basement thrust could not be transferred southwards as in the other two areas, probably because i) the Triassic detachment level was not thick enough for a detachment fold to develop and ii) there are not evaporate levels within the Tertiary sequence of the Ebro basin (except for anhydrite levels shown in cross-section 3-3') allowing for thrust detachment on the south-climbing thrust ramp. Therefore, large-amplitude folds in the Campodarbe Fm. acted as a pin line for the detachment of the Mesozoic-Tertiary cover and displacement was transferred to the North (Fig. 10). Along the cut-off line of the Guarga basement thrust in the study area, the resulting structure is characterized by folds that can be followed for tens of km along trend, but with strong geometrical changes along strike that give a different structure in profile view, at least in detailed cross-sections. This is in contrast with the large-scale structure of the Paleozoic basement, that shows a relatively homogeneous structure consisting in a shallow-dipping thrust probably rooting at deep levels within the crust (Teixell, 1998). The structure of the sedimentary cover is therefore strongly dependent on the mechanical behavior
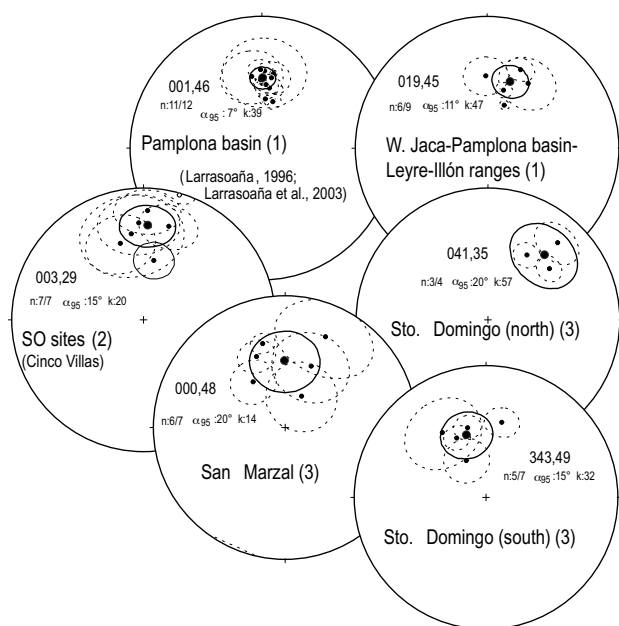
FIGURE 11 | Regional sectors of vertical axis rotations in the studied area after bedding correction. See table 1 and text for more details. n: number of sites. Disontinuous lines represent the alpha 92 for every site of the sector. Continuous lines: represent the alpha 95 for the mean of the sector.

of the different lithologies of the stratigraphic sequence and the position of the detachment levels within it. Structures in the cover relay along strike (see Fig. 10) but shortening is balanced perpendicular to the strike of the structures, which explains the non-rotational character of deformation when considering widespread distributed sampling.

Implications for large-scale rotations in the Pyrenean orogen

The Southern Pyrenees between the South Pyrenean Central Unit and the western termination of the External Sierras have undergone important differences in shortening, which as a result produce clockwise rotations (≈20° in average) as inferred from paleomagnetic data (Oliva-Urcia and Pueyo, 2007a, b). The change of this rotational pattern to a non-rotational pattern at the western termination of the External Sierras can also be established at an orogen-scale in the western sector of the Pyrenees. The western sector of the External Sierras points the limit for this clockwise rotation of the detached Mesozoic-Tertiary cover, thus implying a change in the position of the outermost South-Pyrenean front. This pattern of westward change to non-rotational deformation is also detected in the Pamplona basin (Larrasoaña *et al.*, 2003a), where this change coincides with the meridian defining the western termination of the Axial Zone (with a westward plunge of about 10º; Teixell *et al.*, 2000). According to the results obtained in the External Sierras, this large-scale pattern

can also be explained by 1) the transfer of displacement to different thrusts, located in the hangingwall of the Guarga basement thrust west of the San Marzal pericline, 2) the increasing relevance of south-verging thrusts in the north-Pyrenean Zone (north of the Axial Zone) from East to West, therefore accumulating shortening that eastwards is related to south-verging thrusts in the south-Pyrenean Zone, 3) the general westwards increase of shortening by cleavage formation (Choukroune and Séguret, 1973), 4) the gradual westward decrease of WNW-ESE oriented structures, changing to dominantly E-W oriented structures west of the Pamplona fault (see *e.g.* Larrasoaña *et al.*, 2003a).

CONCLUSIONS

The structural and paleomagnetic investigations of the area west of the Pyrenean External Sierras allow concluding:

The shortening calculated from balancing the three geological cross-sections is 11-13km. The pinning of the Santo Domingo-Tafalla anticline in the westernmost outcrop of the South-Pyrenean Frontal thrust and the increase in thickness of the Campodarbe Fm. to the west restrain the exposure of the South-Pyrenean Frontal thrust in the studied area. The subsurface structure is interpreted as a wedge thrust below the surface expression of the Santo Domingo-Tafalla anticline. The basement thrust sheet interpreted at depth below the main detachment level accommodates 11-13km of shortening and is responsible for uplifting the Mesozoic-Tertiary marine platform deposits to the surface (Leyre-Illón sierras). The structural style depends on the mechanical stratigraphy: the thin limestone units (Mesozoic-Eocene marine platforms) form an imbricated thrust system with low individual displacements and fault-related folds in the hangingwalls of thrusts, whereas the continental deposits of the Campodarbe Fm. behave as a multilayer, the frequency of drag/parasitic folds increasing westwards, in the same sense as the thickness of the whole package and the thinning of the Keuper facies underneath.

The lack of significant differential shortening (constant along-strike for more than 50km) in the area is corroborated with the paleomagnetic study, since no statistically robust vertical axes rotations are found west of the San Marzal pericline. This implies that the apparent changes in the structure at surface correspond rather to relay of fold axes probably related to mechanical stratigraphy than changes driven by vertical axis rotations. The change from rotational to non-rotational kinematics concurs in the meridian including the pinning point of the Santo Domingo anticline and the end of the outcrop of the Pyrenean Axial Zone (shallow westward plunge, north of the studied area).

ACKNOWLEDGMENTS

REFERENCES

Almela, A., Ríos, J.M., 1951. Estudio geológico de la zona subpirenaica aragonesa y de sus sierras marginales. Zaragoza, I Congreso Internacional del Pirineo del Instituto de Estudios Pirenaicos, Geología, 3, 327-350.

Arenas, C., 1993. Sedimentología y paleogeografía del Terciario del margen pirenaico y sector central de la Cuenca del Ebro (zona aragonesa occidental). Doctoral Thesis. Universidad de Zaragoza, Unpublished, 858pp.

Arenas, C., Millán, H., Pardo, G., Pocoví, A., 2001. Ebro Basin continental sedimentation associated with late compressional pyrenean tectonics (NE Iberia): controls on margin fans and alluvial systems. Basin Research, 13, 65-89.

Bailey, R.C., Halls, H. 1984. Estimate of confidence in paleomagnetic directions derived from mixed remagnetization circle and direct observational data. Journal of Geophysics, 54(3), 174-182.

Barnolas, A., Teixell, A., 1994. Platform sedimentation and collapse in a carbonate-dominated margin of a foreland basin (Jaca basin, Eocene, southern Pyrenees). Geology, 22, 1107-1110.

Burbank, D.W., Vergés, J., Muñoz, J.A., 1992. Coeval hindward- and forward-imbricating thrusting in the central southern Pyrenees: timing and rates of shortening and deposition. Geological Society of America Bulletin, 104, 1-18.

Cámara, P., Klimowitz, J., 1985. Interpretación geodinámica de la vertiente centro-occidental surpirenaica (Cuencas de Jaca-Tremp). Estudios Geológicos, 41, 391-404.

Canudo, J.I., Molina, E., Riveline, J., Serra-Kiel, J., Sucunza, M., 1988. Les événements biostratigraphiques de la zone prépyrénéenne d'Aragon (Espagne), de l'Eocène moyen a l'Oligocène inférieur. Revue de Micropaléontologie, 31(1), 15-29.

Capote, R., Muñoz, J.A., Simón, J.L., Liesa, C.L., Arlegui, L.E., 2002. Alpine Tectonics I: The Alpine system north of the Betic cordillera. In: W. Gibbons, W., Moreno, M.T. (eds.). Geology of Spain. London, Geological Society, 385-397.

Casas, A.M., Gil, I., Leránoz, B., Millán, H., Simón, J.L., 1994. Quaternary reactivation of flexural-slip folds by diapiric activity: example from the western Ebro Basin (Spain). Geologische Rundschau, 83, 853-867.

Choukroune, P., Séguret, M., 1973. Carte Structurale des Pyrénées. ELF-ERAP. Mission France. Boussens.

Cuevas, J.L., Marzo, M., Mercadé, L., 1989. Depósitos de barras de meandro de granulometría gruesa en la Formación Talarn (Tránsito mesozoico-cenozoico de la conca de Tremp, Lérida). XII Congreso Español de Sedimentología, Comunicaciones, 19-22.

Faci, E., Castiella, J., García de Domingo, A., del Valle, J., Larrañaga, M.J., 1997. Mapa geológico de Navarra, escala 1:200.000. Gobierno de Navarra, departamento de Obras Públicas, Transportes y Comunicaciones.

Fisher, R.A., 1953. Dispersion on a sphere. Proceedings of the Royal Society of London, A217, 295-305.

Frehner, M., Stefan, M., Schmalholz, S.M., 2006. Numerical simulations of parasitic folding in multilayers. Journal of Structural Geology, 28, 1647-1657.

Hogan, P.J., 1993. Geocrohonologic, tectonic and stratigraphic evolution of the Southwest Pyrenean foreland basin, Northern Spain. Doctoral Thesis. University of Southern California, Unpublished, 219pp.

Hogan, P.J., Burbank, D.W., 1996. Evolution of the Jaca piggyback basin and emergence of the External Sierra, southern Pyrenees. The stratigraphic record of crustal kinematics. Cambridge University Press, E14, 153-160.

Kirschvink, J.L., 1980. The least-squares line and plane and the analysis of paleomagnetic data. Geophysical Journal of the Royal astronomical Society, 62, 669-718.

Labaume, P., Séguret, M., Seyve, C., 1985. Evolution of a turbiditic foreland basin and analogy with an accretionary prism: Example of the Eocene South-Pyrenean basin. Tectonics, 4(7), 661-685.

Lanaja, J.M., 1987. Contribución de la exploración petrolífera al conocimiento de la Geología de España (17 maps). Instituto Geológico y Minero de España, 465pp.

Larrasoaña, J.C., Parés, J.M., Millán, H., del Valle, J., Pueyo, E.L., 2003a. Paleomagnetic, structural and stratigraphic constraints on the traverse fault kinematics during basin inversion: The Pamplona Fault (Pyrenees, north Spain). Tectonics, 22(6), 127-204. doi: 10.1029/2002TC001446.

Larrasoaña, J.C., Parés, J.M., del Valle, J., Millán, H., 2003b. Triassic paleomagnetism from the Western Pyrenees revisited: implications for the Iberian–Eurasian Mesozoic plate boundary. Tectonophysics, 362, 161-182.

Larrasoaña, J.C., Parés, J.M., Pueyo, E.L., 2003c. Stable magnetization carried by magnetite and iron sulphides in marine marls (Pamplona-Arguis formation, Southern Pyrenees, northern Spain). Studia Geophysica et Geodaetica, 47, 237-254.

Larrasoaña Gorosquieta, J.C., Pueyo Morer, E.L., del Valle de Lersundi, J., Millán Garrido, H., Parés, J.M., Pocoví Juan, A., Dinarés Turell, J., 1996. Initial magnetotectonic reports on the Eocene of the Jaca-Pamplona Basin. Geogaceta, 20(4), 1058-1061.

León, I., 1985. Etude sédimentologique et reconstition du cadre géodynamique de le sédimentation détritique fini-Eocène-

Oligocène dans le bassin sud-pyrénéen entre Sangüesa et Pamplona. Doctoral Thesis. Universitée de Pau et des Pays de l'Adour France, 247pp.

Luterbacher, H., 1969. Remarques sur la position stratigraphique de la formation d'Ager (Pyrénées méridionales). Stratigraphic position of the Ager formation, southern Pyrenees. Mémoires du Bureau de recherches géologiques et minières, 69, 225-232.

Martínez-Peña, M.B., Casas-Sainz, A.M. 2003. Cretaceous-Tertiary tectonic inversion of the Cotiella Basin (Southern Pyrenees, Spain). International Journal of Earth Sciences (Geol. Rundsch.). 92: 99-113.

McElhinny, M.W., 1964. Statistical significance of the fold test in paleomagnetism. Geophysical Journal of the Royal Astronomical Society, 8, 338-340.

McElroy, R., 1990. Thrust kinematics and syntectonic sedimentation: the Pyrenean frontal ramp, Huesca, Spain. Doctoral Thesis. University of Cambridge, Unpublished, 175pp.

McFadden, P.L., Lowes, F.J., 1981. The discrimination of mean directions drawn from Fisher distributions. Geophysical Journal of the Royal Astronomical Society, 67, 19-33.

McFadden, P.L., McElhinny, M.W., 1990. Classification of the reversal test in paleomagnetism. In: Mcfadden and McElhinny (eds.), Paleomagnetic Stability and reliability of data. Geophysical Journal International, 103(3), 725-729. (eds.).

Mey, P.H.W., Nagtegaal, P.J.C., Roberti, K.J., Hartevelt, J.J.A., 1968. Lithostratigraphic subdivision of post-hercynian deposits in the south-central Pyrénées, Spain. Leidse Geologische Mededelingen, 41, 221-228.

Millán, H., 1996. Estructura y cinemática del frente de cabalgamiento surpirenaico en las Sierras Exteriores Aragonesas. Doctoral Thesis. Universidad de Zaragoza, 330pp.

Millán, H., Parés, J.M.; Pocoví, A., 1992. Modelización sencilla de la estructura del sector occidental de las sierras marginales aragonesas (Prepirineo, provincias de Huesca y Zaragoza). III Congreso Geológico de España. Simposios, 2, 140-149.

Millán, H.; Pocoví, A. and Casas, A., 1995a. El frente de cabalgamiento surpirenaico en el extremo occidental de las Sierras Exteriores: sistemas imbricados y pliegues de despegue. Revista de la Sociedad Geológica de España, 8(1-2), 73-90.

Millán, H., Den Bezemer, T., Vergés, J., Zoetemeijer, R., Cloething, S., Marzo, M., Muñoz, J.A., Roca E., Cirés, J., 1995b. Paleo-elevation and EET evolution at mountain ranges: inferences from flexural modelling in the Eastern Pyrenees and Ebro Basin. Marine & Petroleum Geology, 12, 917-928.

Millán, H., Pueyo, E., Aurell, M., Luzón, A., Oliva, B., Martínez, B., Pocoví, A., 2000. Actividad tectónica registrada en los depósitos terciarios del frente meridional del Pirineo Central. Revista de la Sociedad Geológica de España. España, 13(2), 279-300.

Millán Garrido, H., 2006. Estructura y Cinemática del frente de cabalgamiento surpirenaico en las Sierras Exteriores. Colección de Estudios Altoaragoneses, 53, 396pp.

Millán Garrido, H., Oliva Urcia, B., Pocoví Juan, A., 2006. The Gavarnie-Guara traverse, Structure and timing of the Gavarnie, Guara-Gèdre and Guarda thrust sheets (Western-Central Pyreenes). Geogaceta, 40, 35-38.

Montes, S., 1992. Sistemas deposicionales en el Eoceno medio-Oligoceno del Sinclinorio de Guarga (cuenca de Jaca, Pirineo central). II Congreso geológico de España. Salamanca 1992, 2, 150-160.

Mutti, E., 1984. The Hecho Eocene Submarine Fan System, South-Central Pyrenees, Spain. Geo-Marine Letters. 3(2-4), 199-202.

Nichols, G. J., 1987. The structure and stratigraphy of the Western External Sierras of the Pyrenees, Northern Spain. Geological Journal, 22(3), 245-259.

Oliva, B., Millán, H., Pocoví, A., Casas, A.M., 1996. Estructura de la Cuenca de Jaca en el sector occidental de las Sierras Exteriores Aragonesas. Geogaceta, 20(4), 800-802.

Oliva, B., Millán, H., Casas, A.M., Pocoví, A., 2000. Estructura del frente pirenaico en el sector occidental de la cuenca de Jaca-Pamplona. Geotemas, 1(1), 75-78.

Oliva-Urcia, B., Pueyo, E.L., 2007a. Gradient of shortening and vertical-axis rotations in the Southern Pyrenees (Spain), insights from a synthesis of paleomagnetic data. Revista de la Sociedad Geológica de España. 20 (1-2), 105-118.

Oliva-Urcia, B., Pueyo, E. L., 2007b. Rotational basement kinematics deduced from remagnetized cover rocks (Internal Sierras, Southwestern Pyrenees). Tectonics, 26 -TC4014.

Ori, G.G., Friend, P.F., 1984. Sedimentary basins formed and carried piggyback on active thrust sheets. Geology, 12, 475-478.

Pocoví, A., Millán, H., Navarro, J.J., Martínez, M.B., 1990. Rasgos estructurales de la Sierra de Salinas y zona de los Mallos (Sierras Exteriores, Prepirineo, Provincias de Huesca y Zaragoza). Geogaceta, 8, 36-39.

Pueyo, E. L., 2000. Rotaciones paleomagnéticas en sistemas de pliegues y cabalgamientos. Tipos, causas, significado y aplicaciones (ejemplos del Pirineo Aragonés). PhD thesis. Universidad de Zaragoza, 296pp.

Pueyo, E.L., Parés, J.M., Millán, H., Pocoví. A., 1994. Evidencia magnetotectónica de la rotación de la Sierras Exteriores Altoaragonesas. Comunicaciones del II Congreso Grupo Español del Terciario (Jaca), 185-188.

Pueyo, E.; Millán, H.; Pocoví, A., Parés, J.M, 1999. Cinemática rotacional del cabalgamiento basal surpirenaico en las Sierras Exteriores Aragonesas: Datos magnetotectónicos. Acta Geológica Hispánica, 32(3-4), 237-256.

Pueyo, E.L., Millán, H., Pocoví, A., 2002. Rotation velocity of a thrust: a paleomagnetic study in the External Sierras (Southern Pyrenees). Sedimentary Geology, 146(1-2), 191-208

Pueyo, E.L., Pocoví, A., Parés, J.M., Millán, H., Larrasoaña, J.C., 2003a. Thrust ramp geometry and spurious rotations of paleomagnetic vectors. Studia Geophys. Geod., 47(2), 331-357.

Pueyo E. L., Parés, J.M., Millán, H., Pocoví A., 2003b. Conical folds and apparent rotations in paleomagnetism (A case study in the Pyrenees). Tectonophysics, 362 (1/4), 345-366.

Pueyo E. L., Pocoví, A., Millán, H., Sussman. A.J., 2004. Map view model to correct and calculate shortening in rotated thrust fronts using paleomagnetic data. In: Paleomagnetic and structural analyses of orogenic curvature (A. J. Sussman and A. B. Well, Eds.). Geological Society of America (Special Publications), 383: 57-71.

Puigdefábregas, C., 1975. La sedimentación molásica en la cuenca de Jaca. Pirineos, 104, 1-188.

Ramberg, H., 1963. Fluid dynamics of viscous buckling applicable to folding of layered rocks. Bulletin of the American Association of Petroleum Geologits, 47(3), 484-505.

Ramón, M.J., Pueyo, E.L., 2008. Cálculo de direcciones y planos virtuales paleomagnéticas: ejemplos y comparación con otros métodos. Geotemas, 10, 1203-1206.

Ramsay, J. G., 1974. Development of chevron folds. Geol. Soc. Am. Bull., 85, 1741-1754.

Ramsay, J. G., Huber M. I., 1987. The techniques of modern structural geology. Volume 2: Folds and fractures. Academic Press Limited.

Scheepers, P.J.J., Zijderveld J.D.A. 1992. Stacking in paleomagnetism; application to marine sediments with weak NRM. Geophysical Research Letters, 19(14), 1519-1522.

Séguret, M., 1972. Etude tectonique des nappes et séries décollées de la partie centrale du versant sud des Pyrénées. Caractère synsédymentaire, rôle de la compression et de la gravité. Thèse Fac. Sc. de Montpellier (1970). Publ. de l'Univ. des Sc. et Tec. du Languedoc (USTELA), Sér. Geol. Struct., nº 2, 155pp.

Soler, M., Puigdefàbregas, C., 1970. Líneas generales de la geología del Alto Aragón Occidental. Pirineos, 96, 5-20.

Soto, R., Casas-Sainz, A.M., Pueyo, E.L., 2006. Along-strike variation of orogenic wedges associated with vertical axis rotations. Journal of Geophysical Research. Res. 111 (B10) Article Number: B10402.

Suppe, J., 1983. Geometry and kinematics of fault-bend folding. American Journal of Science, 283(7), 684-721.

Taberner, C., Dinarès-Turell, J., Giménez, J., Docherty, C., 1999. Basin infill architecture and evolution from magnetostratigraphic cross-basin correlations in the southern Pyrenean foreland basin. Geological Society of American Bulletin, 111, 1155-1174.

Teixell, A., 1992. Estructura alpina en la transversal de la terminación occidental de la Zona Axial pirenaica. Tesis doctoral. Univ. de Barcelona., 252pp.

Teixell, A., 1996. The Ansó transect of the southern Pyrenees: basement and cover thrust geometries. Journal of Geophysical Research, 102, 20325-20342.

Teixell, A., 1998. Crustal structure and orogenic material budget in the west central Pyrenees. Tectonics, 17(3), 395-406.

Teixell, A., García-Sansegundo, J., 1995. Estructura del sector central de la Cuenca de Jaca (Pirineos Meridionales). Revista de la Sociedad Geológica de España, 8(3), 215-228.

Teixell, A., Durney, D.W., Arboleya, M.L., 2000. Stress and fluid control on decollement within competent limestone. Journal of Structural Geology, 22(3), 349-371.

Torsvik, T., Briden, J., Smethurst, M. 1996. SuperIAPD software. http://www.geodynamics.no/software.htm.

Turner, J.P., Hancock, P.L., 1990. Relationships between thrusting and joint systems in the Jaca thrust-top basin. Spanish Pyrenees. Journal of Structural Geology, 12, 217-226.

Van der Voo, R., 1993. Paleomagnetism of the Atlantic, Tethys and Iapetus ocean. Cambridge University Press, 411pp.

Electronic appendix

TABLE 1 | Paleomagetic data of every site. Numbers indicate the position of the site in Fig. 3. Previously published (unpublished) data are the numbers without (with) apostrophe. UTM Coordinates of every site. Max and Min are the maximum and minimum stratigraphic age in millions years. Bedding plane with strike (DD) and dip. (*) indicates great circles and intersections with PCA analyses for the mean calculation method, (**) indicates the addition of the stacked sample to these methods. n/N number of samples used for the mean calculation. In situ declination (Dec) and inclination (Inc) with the statistical parameters (α95 and k). The same data for the bedding corrected mean. β is the rotation respect to the reference Taberner *et al* (1999)

#	Site	Reference	UTM (E-W)	UTM (N-S)	Formation	Stratigraphic Age	Max	Min	Strike	Dip	DD	Sector
1	Bagües N	Hogan, 1993; Hogan & Burbank, 1996	668199	4712316	Campodarbe	Upper Eocene-Oligocene	37.2	23	90	24	S	Western Jaca basin- Leyre Illón ranges (1)
2	Bagües R	Hogan, 1993; Hogan & Burbank, 1996	668199	4712316	Campodarbe	Upper Eocene-Oligocene	37.2	23	65	29	SE	Western Jaca basin- Leyre Illón ranges (1)
3	SI01	Larrasoaña et al., 1996	649830	4720520	Arro-Fiscal	Lutetian-Cuisian	52.7	41.5	112	12	S	Western Jaca basin- Leyre Illón ranges (1)
4	ST01-A	Larrasoaña et al., 1996	662772	4728174	Hecho	Lutetian-Cuisian	52.7	41.5	107	51	S	Western Jaca basin- Leyre Illón ranges (1)
5	ST01-B	Larrasoaña et al., 1996	662772	4728174	Hecho	Lutetian-Cuisian	52.7	41.5	300	14	N	Western Jaca basin- Leyre Illón ranges (1)
6	BE01	Larrasoaña et al., 1996	675400	4718910	Sabiñanigo	Lower Bartonian	40.1	39.6	27	18	E	Western Jaca basin- Leyre Illón ranges (1)
7	LI01	Larrasoaña et al., 1996	641847	4720620	Pamplona-Arguis marls (Urroz mbr.)	Bartonian-Priabonian	40	34.1	258	82	NW	Pamplona basin (1)
8	LU01	Larrasoaña et al., 1996	639132	4723244	Pamplona-Arguis marls (Urroz mbr.)	Bartonian-Priabonian	40	34.1	283	26	NE	Pamplona basin (1)
9	LI02	Larrasoaña et al., 2003	638446	4719929	Pamplona-Arguis marls (Urroz mbr.)	Bartonian-Priabonian	40	34.1	106	45	S	Pamplona basin (1)
10	LI03	Larrasoaña et al., 2003	637684	4720407	Pamplona-Arguis marls (Urroz mbr.)	Bartonian-Priabonian	40	34.1	224	9	NE	Pamplona basin (1)
11	LI04	Larrasoaña et al., 2003	638676	4720952	Pamplona-Arguis marls (Urroz mbr.)	Bartonian-Priabonian	40	34.1	272	27	N	Pamplona basin (1)
12	LI05	Larrasoaña et al., 2003	639710	4719429	Pamplona-Arguis marls (Urroz mbr.)	Bartonian-Priabonian	40	34.1	96	85	S	Pamplona basin (1)
13	LI06	Larrasoaña et al., 2003	638313	4720914	Pamplona-Arguis marls (Urroz mbr.)	Bartonian-Priabonian	40	34.1	304	14	NE	Pamplona basin (1)
14	LU02	Larrasoaña et al., 2003	641609	4723541	Pamplona-Arguis marls (Urroz mbr.)	Bartonian-Priabonian	40	34.1	272	32	N	Pamplona basin (1)
15	LU03	Larrasoaña et al., 2003	644086	4723839	Pamplona-Arguis marls (Urroz mbr.)	Bartonian-Priabonian	40	34.1	179	21	N	Pamplona basin (1)
16	LU04	Larrasoaña et al., 2003	640530	4727315	Pamplona-Arguis marls (Urroz mbr.)	Bartonian-Priabonian	40	34.1	157	22	SW	Pamplona basin (1)
17	LU05	Larrasoaña et al., 2003	642110	4735711	Pamplona-Arguis marls (Urroz mbr.)	Bartonian-Priabonian	40	34.1	106	28	S	Pamplona basin (1)
18	RI01	Larrasoaña et al., 2003	638231	4729553	Pamplona-Arguis marls (Urroz mbr.)	Bartonian-Priabonian	40	34.1	129	28	SW	Pamplona basin (1)
19	SD07	Pueyo et al., 2003a	676148	4697379	Arguis-Pamplona	Bartonian	40.5	37	117	100	S	Western External Sierras (3)
20	VL01	Pueyo et al., 2003a	674452	4699900	Yeste-Arrés	Upp. Bartonian	37	36.6	317	84	E	Western External Sierras (3)
21	VL03	Pueyo et al., 2003a	673049	4701150	Yeste-Arrés	Upp. Bartonian	37	36.6	322	78	E	Western External Sierras (3)
22	VL04	Pueyo et al., 2003a	682150	4698080	Arguis-Pamplona	Bartonian	40.5	37	290	82	N	Western External Sierras (3)
23	VL02	Pueyo et al., 2003a	676700	4699110	Arguis-Pamplona	Bartonian	40.5	37	83	63	N	Western External Sierras (3)
24	AR06	Pueyo et al., 2004	666850	4703470	Arguis-Pamplona	Bartonian	40.5	37	199	63	W	Western External Sierras (3)
25	SM01	Pueyo et al., 2004	667955	4703275	Arguis-Pamplona	Bartonian	40.5	37	275	77	N	Western External Sierras (3)
1'	SM02	Pueyo, 2000	667000	4703053	Arguis-Pamplona	Bartonian	40.5	37	152	57	W	Western External Sierras (3)
2'	SM03	Pueyo, 2000	667000	4703230	Arguis-Pamplona	Bartonian	40.5	37	160	77	W	Western External Sierras (3)
3'	SM04	Pueyo, 2000	667425	4703550	Arguis-Pamplona	Bartonian	40.5	37	260	71	N	Western External Sierras (3)
4'	SM05	Pueyo, 2000	667180	4703423	Arguis-Pamplona	Bartonian	40.5	37	229	68	N	Western External Sierras (3)
5'	SM06	Pueyo, 2000	666703	4703000	Arguis-Pamplona	Bartonian	40.5	37	157	80	W	Western External Sierras (3)
6'	SD01	Pueyo, 2000	666979	4702766	Arguis-Pamplona	Bartonian	40.5	37	127	96	S	Western External Sierras (3)
7'	SD02	Pueyo, 2000	668463	4702130	Arguis-Pamplona	Bartonian	40.5	37	127	96	S	Western External Sierras (3)
8'	SD03	Pueyo, 2000	667305	4702380	Arguis-Pamplona	Bartonian	40.5	37	117	106	S	Western External Sierras (3)
9'	SD04	Pueyo, 2000	669695	4701418	Arguis-Pamplona	Bartonian	40.5	37	131	42	S	Western External Sierras (3)
10'	SD05	Pueyo, 2000	672005	4700150	Arguis-Pamplona	Bartonian	40.5	37	127	94	S	Western External Sierras (3)
11'	SD06	Pueyo, 2000	673500	4698843	Arguis-Pamplona	Bartonian	40.5	37	118	91	S	Western External Sierras (3)
12'	LN01	Pueyo, 2000	670440	4705850	Campodarbe III	Rupelian	34.2	28.7	323	54	E	Western External Sierras (3)
13'	YS01	Pueyo, 2000	649830	4720520	Arguis-Pamplona	Bartonian	40.5	37	92	33	S	Western Jaca basin- Leyre Illón ranges (1)
14'	RU01	Pueyo, 2000	657790	4717600	Liédena	Upp. Bartonian	37	36.6	95	29	S	Western Jaca basin- Leyre Illón ranges (1)
15'	MI01	Pueyo, 2000	667870	4716960	Arguis-Pamplona	Bartonian	40.5	37	96	32	S	Western Jaca basin- Leyre Illón ranges (1)
16'	SO01	Pueyo, 2000	648407	4703468	Bernués	Rupelian-Chattian	31	27	99	14	S	Cinco Villas section (2)
17'	SO02	Pueyo, 2000	647607	4708364	Campodarbe III	Rupelian	34.2	28.7	104	82	S	Cinco Villas section (2)
18'	SO03	Pueyo, 2000	651660	4708200	Campodarbe III	Rupelian	34.2	28.7	114	57	S	Cinco Villas section (2)
19'	SO04	Pueyo, 2000	654270	4710730	Campodarbe II	Rupelian	34.2	28.7	112	100	S	Cinco Villas section (2)
20'	SO05	Pueyo, 2000	652380	4708950	Campodarbe II	Rupelian	34.2	28.7	90	78	S	Cinco Villas section (2)
21'	SO06	Pueyo, 2000	655000	4708920	Campodarbe II	Rupelian	34.2	28.7	296	57	N	Cinco Villas section (2)
22'	SO07	Pueyo, 2000	654480	4713540	Campodarbe II	Rupelian	34.2	28.7	15	59	E	Cinco Villas section (2)

TABLE I | Continued

#	Structure	Method	n	N	In situ (btc) Dec	Inc	α₉₅	k	After tectonic correction (atc) Dec	Inc	α₉₅	k	β
1	Bailo syn. - Atarés ant.	PCA	3	3	8	-4	4	129	8	20	4.6	109	3
2	Bailo syn. - Atarés ant.	PCA	30	30	190	7	9	10	191	-17	8.9	11	6
3	Atarés ant.-Bailo syn.	PCA	9	9	20	40	5	128	16	52	5	128	11
4	Illón (Jaca) thrust	PCA	9	9	202	16	8	38	203	-35	8	38	18
5	Illón (Jaca) thrust	PCA	9	9	201	-50	8	38	203	-35	8	38	18
6	Atarés ant. N	PCA	11	11	350	34	13	13	359	44	13	13	-6
7	Liédena ant.	PCA	9	9	221	84	11	21	343	12	11	21	-22
8	Lumbier syn.	PCA	9	9	5	68	1.9	722.3	9	42	1.9	722.3	4
9	Liédena ant.	PCA	6	8	359	1	17.9	15.0	352	44	17.9	15.0	-13
10	Liédena ant.	PCA	5	8	9	47	23.6	11.5	2	41	23.6	11.5	-3
11	Liédena ant.	PCA	8	8	15	72	10.6	28.3	8	45	10.6	28.3	3
12	Liédena ant.	PCA	8	10	5	-26	3.9	203.4	4	59	3.9	203.4	1
13	Liédena ant.	PCA	10	10	358	72	4.5	114.2	13	60	4.5	114.2	10
14	Lumbier syn.	PCA	8	8	355	81	4.5	151.3	0	49	4.5	151.3	-3
15	Lumbier syn.	PCA	9	9	16	37	6.7	59.3	359	40	6.7	59.3	-4
16	Lumbier syn.	PCA	8	8	16	36	3.3	289.7	359	47	3.3	289.7	-4
17	Lumbier syn.	PCA	9	10	10	24	8.2	40.9	7	52	8.2	40.9	2
18	Lumbier syn.	PCA	9	10	15	25	6.5	63.6	4	50	6.5	63.6	-1
19	Sto. Domingo ant. S	PCA	7	7	9	-56	10	33	12	41	10	33	7
20	Sto. Domingo ant. N	PCA	10	11	226	57	8	56	50	39	8	56	45
21	Sto. Domingo ant. N	PCA	6	11	279	76	13	22	42	22	13	22	37
22	Sto. Domingo ant. N	PCA	9	9	188	55	8	36	31	42	8	36	26
23	Fachar-Sto. Domingo ant.	PCA(**)	10	10	177	74	11	6	15	43	11	6	10
24	San Marzal pericline	PCA(**)	25	25	45	42	7	19	345	34	7	19	-20
25	San Marzal pericline	PCA	14	17	296	62	33	<1	338	3	33	<1	-27
1'	San Marzal pericline	PCA	7	9	40	-2	23	7	23	48	23	7	18
2'	San Marzal pericline	PCA	9	10	203	-10	11	22	158	-41	11	22	-27
3'	San Marzal pericline	PCA(*)	2	4	280	-58	27	43	204	-25	27	43	19
4'	San Marzal pericline	PCA(*)	4	4	299	-28	22	14	208	-68	22	14	23
5'	San Marzal pericline	PCA	10	10	34	15	14	11	325	55	14	11	-40
6'	Sto. Domingo ant. S	PCA	5	8	350	-18	23	10	326	40	23	10	-39
7'	Sto. Domingo ant. S	PCA	2	2	233	68	>40	5	222	-27	>40	5	37
8'	Sto. Domingo ant. S	PCA	6	10	6	-29	14	19	332	64	14	19	-33
9'	Sto. Domingo ant. S	PCA	4	4	12	19	35	6	348	51	35	6	-17
10'	Sto. Domingo ant. S	PCA	8	10	360	-21	8	43	334	48	8	43	-31
11'	Sto. Domingo ant. S	PCA	7	8	355	-33	8	45	345	44	8	45	-20
12'	Longás syn.	PCA	8	8	141	-42	22	6	177	-27	22	6	-8
13'	Atarés ant.-Bailo syn.	PCA	10	10	16	29	3	184	22	61	3	184	17
14'	Atarés ant.-Bailo syn.	PCA	7	8	29	14	17	11	32	41	17	11	27
15'	Bailo syn. - Atarés ant.	PCA	4	5	15	49	8	111	30	80	8	111	25
16'	Tafalla-Sos ant.	PCA	6	7	357	20	29	5	352	34	29	5	-13
17'	Tafalla-Sos ant.	PCA	9	10	36	-24	18	9	43	53	18	9	38
18'	Urriés-Navardún ant.	PCA	6	8	176	9	20	10	163	-39	20	10	-22
19'	Undués-Botaya ant.	PCA	9	9	194	47	12	11	190	-52	12	11	5
20'	Urriés-Navardún ant.	PCA	6	7	203	48	16	16	195	-27	16	16	10
21'	Urriés-Navardún ant.	PCA	15	15	192	-55	7	29	196	1	7	29	11
22'	Undués-Botaya ant.	PCA	7	9	356	-2	17	12	2	18	17	12	-3